

PCCP

Accepted Manuscript



This is an *Accepted Manuscript*, which has been through the Royal Society of Chemistry peer review process and has been accepted for publication.

Accepted Manuscripts are published online shortly after acceptance, before technical editing, formatting and proof reading. Using this free service, authors can make their results available to the community, in citable form, before we publish the edited article. We will replace this *Accepted Manuscript* with the edited and formatted *Advance Article* as soon as it is available.

You can find more information about *Accepted Manuscripts* in the [Information for Authors](#).

Please note that technical editing may introduce minor changes to the text and/or graphics, which may alter content. The journal's standard [Terms & Conditions](#) and the [Ethical guidelines](#) still apply. In no event shall the Royal Society of Chemistry be held responsible for any errors or omissions in this *Accepted Manuscript* or any consequences arising from the use of any information it contains.

Density Functional Studies on $(\text{NCH})_n$ AzaGraphane: Activated Surface for Organocatalysis

Cite this: DOI: 10.1039/x0xx00000x

S. Marutheeswaran,^a Pattath D. Pancharatna^a and Musiri M. Balakrishnarajan^{a*}

Received 00th June 2014,
Accepted 00th June 2014

DOI: 10.1039/x0xx00000x

www.rsc.org/

Quantum chemical analysis shows aza-graphane isomers, with alternate C-H and N: sites as ideal organocatalysts; its kinetic stability arises from the tertiary orthoamide. DFT calculations give split-off bands originating from nitrogen lone-pairs with substantial mixing of hydrogen, indicating an optimal balance between nitrogen basicity and C-H activation through anomeric effect.

The experimental characterization of graphane¹ and fluorographane² nanosheets, though not isolated in pure form,³ arouse substantial interest in characterizing its analogues for a variety of promising applications. An interesting possibility is the isoelectronic replacement of selected C-H groups of the graphane with a lone pair bearing nitrogen (N:). Since the σ -bond strength of C-N (~73 kcal/mol) is twice that of N-N (~38 kcal/mol), the thermodynamically most stable structures would naturally prefer C-N bonds. Hence, an alternating network of N: and C-H groups with the composition $(\text{NCH})_n$ is a potential possibility. This $(\text{NCH})_n$ nanosheet, which we refer to as 'azagraphane' (Figure 1.a), may be kinetically more stable than graphane, as its competing phase of dehydrogenated graphene analogue (Figure 1b) is not neutral.

In addition to the chemical functionality arising from the N: lone pair,⁴ the C-H bonds in these azagraphanes could be immensely activated by the appropriately oriented lone pairs of the three surrounding nitrogen atoms through anomeric effect.⁵ This polarizes the C-H bonds imparting hydridic nature,⁶ similar to that of a hydrogenated metal surface. The C-H group environment, as found in cyclic orthoamides, are known to be stable only in the absence of hydrogen atoms in the nitrogen⁷ (*i.e.*, tertiary amino groups) without which they rapidly lose hydride ion to form the guanidinium salts. This is ideally satisfied in the alternating $(\text{NCH})_n$ network where N is tertiary in nature. The activated C-H groups may still readily lose

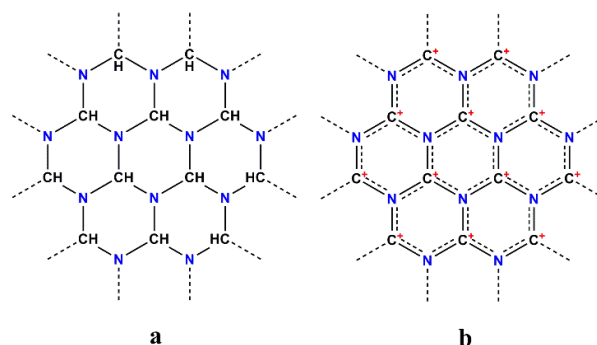


Figure 1. The nanosheets of (a) azagraphane and (b) its dehydrated graphene analogue

hydride ion under acidic conditions as observed in the cyclic orthoamides.⁵

The electrophilic C^+ sites on the resulting surface are separated by just one nitrogen making it the two-dimensional analogue of the gitonic 1, 3-superelectrophiles.⁸ Further, the presence of both acidic and basic sites in the dehydrated surface effectively mimics the metal oxide surface. This raises the scope of azagraphanes as metal free organocatalysts in which the carbocation site mimics the metal as Lewis acid while the lone pair bearing nitrogen mimics the oxygen atom as Lewis bases. Due to the cyclic orthoamide motif, azagraphanes are also potential candidates for hydrogen storage/evolution under acidic conditions,⁵ metal free reduction mimicking the enzymes,^{9,10} DNA cleavage properties¹¹ and a host of other applications related to super-electrophiles.

Azagraphanes are viable for experimental characterization either by rational synthetic methods like polymerization of the appropriately functionalized monomers (*i.e.*, triazinane derivatives) or from heavily nitrogen doped graphene by strategies involving insertion of C-H group in the cavity of the aza-macrocyclic.¹² Predictions based on

quantum mechanical simulations show that HCN molecular crystal under high pressure and favourable temperatures may lead to a polymeric solid that has stacking of azagraphane layers.¹³

The possibility of rational synthesis and a host of promising applications make azagraphanes potential targets for synthesis. However, different conformational isomers are possible for azagraphanes, based on the orientation of the lone pair and the C-H groups. The relative stability of these conformers and the nature of preferred anomeric delocalization for the N: lone pair determines the critical question about the reactivity of their surface. The comparative stability of various conformers also give an estimate of the relative basicity^{14,15} of the C-H groups as the conjugate acid for all the conformers is unique and isoelectronic to graphene (Figure 1b). Since graphene itself is known to have several conformations,³ the free energy surface of azagraphane indeed is expected to be complex. Here, we theoretically explore the structure, stability and bonding of various isomeric azagraphane frameworks, their electronic band structure and nature of frontier levels using DFT calculations.

We started with investigating the stabilities of graphane conformers, as several of them are reported independently and the stereoelectronic factors that determine their stability ordering are not collectively discussed in detail.¹⁶⁻²¹ We computed the six most stable isomers (Figure 2); they all have only one type of six membered ring but differ in hydrogen orientation. For clarity, they are labelled with their respective 2D-space symmetry along with their common names. The symmetrically distinct C-C bonds and the associated H-C-C-H dihedral angle are employed to assess their relative stability. As seen from figure 2, the dihedral angle variation (180° to 0°), correlates well with C-C bond lengths and they collectively determine the stability of the conformer. The three most stable conformers have carbon rings in chair form, followed by the next two in boat form; the twist-boat skeleton is the least stable, as is expected from steric factors. These results agree with the earlier reports¹⁶⁻²¹ and other isomers having multiple non-equivalent hexagonal rings are ignored as they are high in energy.¹⁹

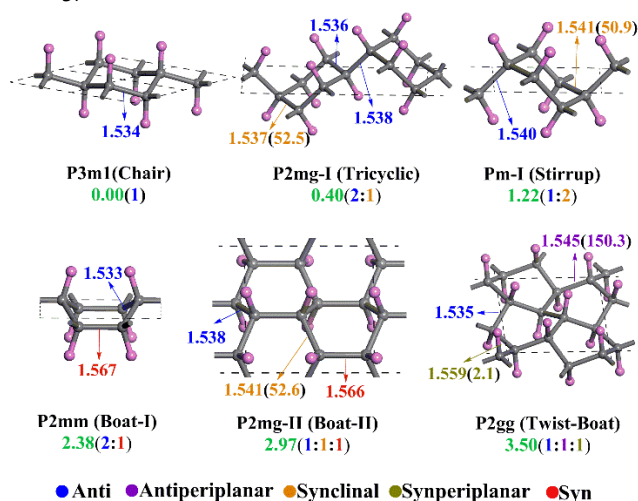


Figure 2. The most stable conformers of graphane with their 2D-space symmetry along with their common names (in brackets). The relative energies (kcal/mol per CH group) is shown in green with the ratio (per unit cell) of various possible stereochemical orientation (coloured distinctly) of hydrogens across C-C bonds. The corresponding dihedral angle ($^\circ$) is given along with C-C distances (Å).

The observed stability ordering is better understood based on the substitutional preferences of the cyclohexane conformers. The thermodynamically most stable conformer ($P3m1$), generally referred as 'chair',²⁷ has a distinct hexagonal lattice ($Z=2$) with all hydrogen atoms occupying axial positions. This favourably keeps all the bulky carbon atoms equatorial and also forces anti orientation between every adjacent C-H groups. But the energetically close $P2mg-I$ (tricyclic²⁵) conformer has one of the carbon atoms axial, causing instability. The reduced symmetry results in a larger unit-cell ($Z=8$) in which one-third of the adjacent C-H bonds are synclinal forced by the axial carbon atoms. The next stable stirrup¹⁸ isomer ($Pm-I$) has two of the carbon atoms axial, leading to further destabilization. As they occur at 1, 4 – positions, the unit cell size is reduced ($Z=4$); but two-third of adjacent hydrogen atoms turn synclinal. The next $P2mm$ isomer²⁷ ($Z=4$) has one-third of the C-C bonds in unfavourable eclipsed orientation due to the boat geometry that forces syn alignment between C-H bonds. The second boat isomer¹⁹ $P2mg-II$ ($Z=8$) has two of the carbon atoms axial (or flagpole) making it further unstable in which the number of favourable anti C-H orientations are reduced to one-third. The final structure ($Z=8$) has the chiral $P2gg$ symmetry with twist-boat conformation²⁰ which is destabilizing due to more number of C-C bonds in unfavourable stereo environment. Thus the thermodynamic stabilities of the conformers correlate well with the number and nature of orientation of hydrogens (Figure 2), which is a consequence of their topology.

For each one of these graphane isomers, substitution of alternate C-H groups with the isoelectronic N: should lead to different isomers of azagraphane. However all isomers except $P2mg-I$, have only one type of C-H group. Also, for $P2mg-I$ conformer, though there are two symmetrically distinct C-H groups, one of them is connected to its own type. So only one azagraphane isomer is possible with alternating carbon-nitrogen network for each of the graphane isomers. The optimized geometry of these six azagraphane isomers is given along with their band structure and projected density of states of individual atoms in Figure 3. The stereochemistry associated around the distinct C-N bonds are given with reference to the lone pair orientation of the nitrogen and C-H bonds. Here, the orientation of N: lone pair is assumed to be coplanar to the vector that passes in between the two other substituents of the nitrogen atom. The anomeric delocalization strengthens the C-N π bonding at the expense of weakening the σ -bond that is antiperiplanar to the N: lone pair ($n \rightarrow \pi^*$ donation). The energetic proximity and effectiveness of overlap between the lone pair (n) and antiperiplanar σ^* fragment MOs will determine the energetic preferences.

The hexagonal $P3m1$ graphane conformer retains its symmetry even after one of the C-H groups is replaced by N: in azagraphane. Compared to the ideal C-H (1.10 Å) and C-N (1.47 Å) single bond distances, C-H bonds are elongated by ~ 0.05 Å while C-N bonds are shortened by 0.015 Å since the C-H bonds are aptly oriented for anomeric delocalization of N: lone pair. The pyramidalization angle²² of nitrogen, computed as the deviation of the sum of all the three C-N-C angles from 360° around the nitrogen, also shows flattening by 11° (compared to the ideal value of 42° in NH_3) due to partial C-N π -bonding.

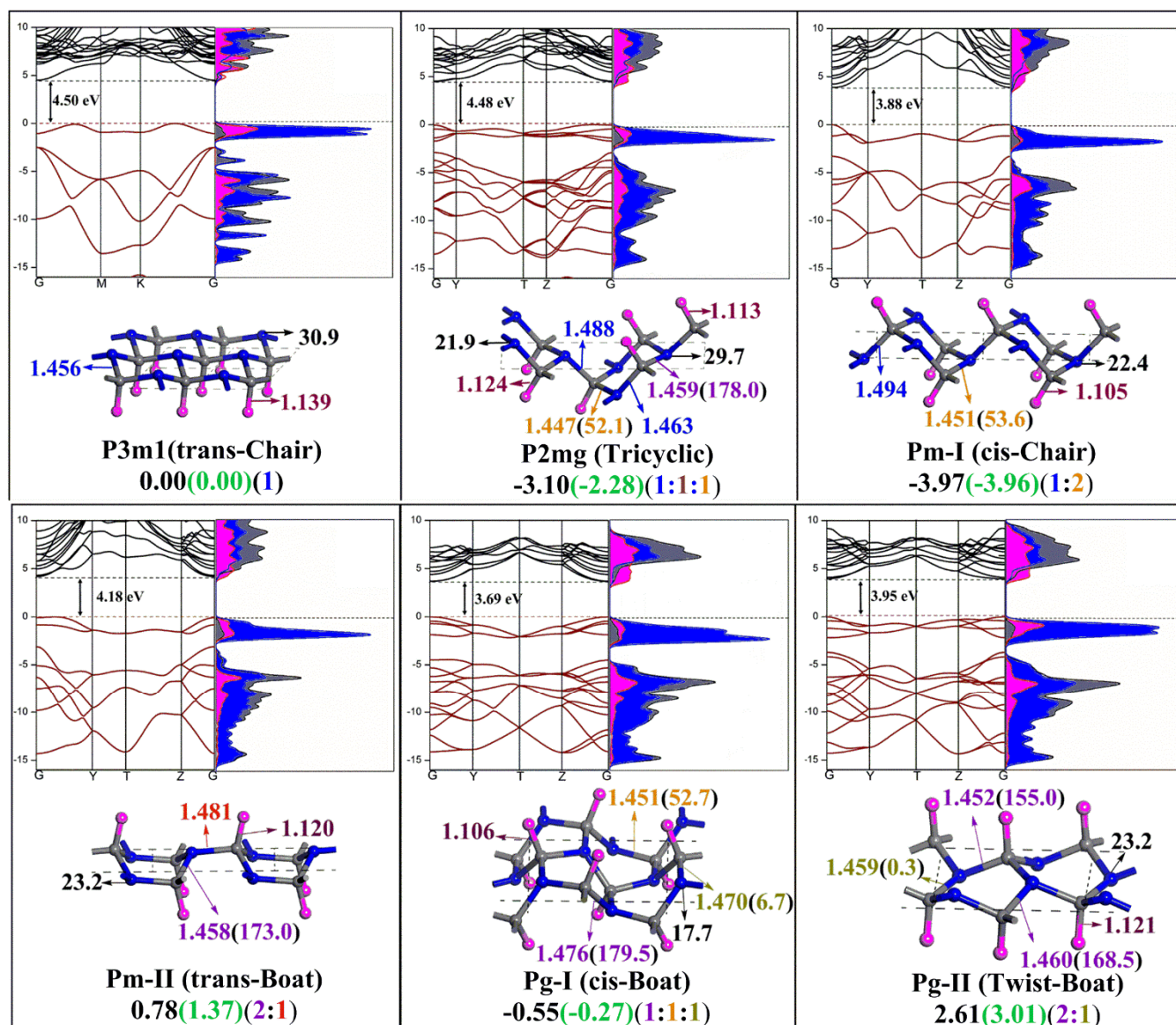


Figure 3. The azagraphane conformers with their 2D-space symmetry and relative energies at GGA (and LDA) with respect to chair form. The bond lengths, dihedral angles and the ratio of various stereo orientations between N: lone pair and H follow the same colouring as of Figure 2. Pyramidalization angles around N is given in black. The band structure (left) and projected DOS (right) of individual elements with their respective colours are given above the respective structures.

The computed band structure shows a large band-gap (Figure 3), the conduction band minimum is at G while the valence band maximum lies in between G and K special k-points.

In the frontier, the top of the valence band has a split-off band separated from the rest of valence bands by more than 1 eV and spread over by 0.75 eV. Projected density of states of individual atoms show that this band arise predominantly from N: lone pair. The definite gap between the split-off band and the rest of the filled bands indicates substantial reactivity of the N: lone-pairs. There is also definite mixing of H and C DOS in this band due to anomeric effect and the increased presence of the former in this region clearly reveals the increased basicity of hydrogen atoms. The bottom of the conduction band has predominant contribution from H and C as these are mainly C-H antibonding in this isomer.

The tricyclic P2mg-I conformer also retains its symmetry, but is more stable than P3m1 isomer by ~3kcal/mol per formula unit. Among the two distinct nitrogen atoms, one N: lone pair is anti to one adjacent C-H bonds while other two C-H bonds are slightly deviated (antiperiplanar). The other N: lone pair is antiperiplanar to two C-N bonds (synclinal to C-H) and anti to one C-H bond. The dihedral angle between the lone pair and its antiperiplanar σ -bond determines the efficiency of the anomeric effect. Due to this subtle change, the C-H bond that has less anomeric delocalization is slightly shorter than the other. Similarly there are two short C-N bonds that host $n \rightarrow \sigma^*_{C-H}$ effect and other two C-N bond are longer due to $n \rightarrow \sigma^*_{C-N}$. Its band structure shows indirect band gap similar to P3m1, and there are split-off bands that correspond to four N: lone pairs in the unit cell that are comparatively wider but with reduced hydrogen mixing as expected.

The increased stability of this isomer compared to the chair form indicates that anomeric delocalization of the N: lone pair over σ^*_{C-N} is energetically preferred over σ^*_{C-H} . The increased anomeric delocalization in this isomer compared to the chair form is also reflected in the increased flattening of one of the nitrogen atom that hosts σ^*_{C-N} delocalization indicated by the substantially reduced pyramidalization angle.

The stirrup (Pm-I) conformer also retains its symmetry like other two chair forms and is thermodynamically the most stable among all the computed structures. The increased stability can be attributed to the delocalization of N: lone pair to two antiperiplanar σ^*_{C-N} bonds and one anti σ^*_{C-H} bonds. The pyramidalization angle of nitrogen shows substantial flattening and the pronounced anomeric delocalization is also reflected in the band structure that exhibits reduced, but direct band gap at G. The valence bands are pushed down while moving away from G, exhibiting a larger width for the split-off bands arising from the two N: lone pairs.

The P2mm conformer of graphane loses its C₂ axis and one of its mirror plane in its azagraphane analogue, reducing its symmetry to Pm (Pm-II). Here, the N: lone pair is antiperiplanar to two of the C-H bonds and syn to one of the C-H bond which facilitates exclusively $n \rightarrow \sigma^*_{C-H}$ donation and makes the structure comparable to P3m1 isomer. The other boat conformer of graphane P2mg-II also loses its C₂ axis and mirror plane reducing to Pg in its aza-graphane form. However, the N: lone pair here is antiperiplanar to one C-H bond and one C-N bond that adds substantial stability. Hence this structure is found to be marginally more stable compared to P3m1, despite having the destabilizing syn interactions inherent in its boat conformation. The magnitude of the band gap and nature of the bands/projected density of states of these boat-forms corroborates the observed stability ordering. The azagraphane structure derived from twist-boat retains its Pg symmetry and its N: lone pair is antiperiplanar to two C-H bonds but with larger deviations. The other C-H bond is not appropriately oriented to exert anomeric effect due to the inherent symmetry of the twist-boat conformation. Hence it remains the least stable among all the structures considered here.

The computed Mülliken charges (Table 1) of various azagraphanes reflects the extent of hydridic nature arising from anomeric effect. Compared to graphane, all the azagraphane conformers have reduced Mülliken charges on hydrogens with the P3m1 isomer having substantial reduction as it involves maximum delocalisation of lone-pair to σ^*_{C-H} . For comparison, we also computed the charges on hydrogen for a molecular cyclic orthoamide (perhydro - 3a, 6a, 9a - triazaphenalene) in which nitrogen lone pairs are anti-periplanar to C-H. As seen from Table 1, the charges on C and H are comparable to the P3m1 isomer. ¹H NMR values (Table 1) also show an upfield chemical shift for P3m1 compared to graphane indicative of electronic shielding. This is similar to its molecular counterparts where methyl proton has a chemical shift of 0-2 ppm and orthoamide 2.25 ppm. Since the spatial screening of nitrogen lone pairs also affect the NMR values,¹⁵ there are other azagraphane isomers, especially the boat forms with even lower chemical shifts. Hence, Mülliken charges turn out to be a better indicator for assessing the hydridic nature of C-H.

Table 1. Mülliken charges and absolute NMR values (iso) of azagraphane isomers are given. Graphane and a molecular cyclic orthoamide are included for comparison.

	Mülliken charge			NMR(ppm)		
	C	N	H	C	N	H
Graphane	-0.45	-	0.45	121.4	-	30.4
P3m1	0.14	-0.28	0.14	80.0	160.7	27.6
P2mg	0.13 0.10	-0.33 -0.36	0.20 0.27	87.0 85.9	162.2 159.1	26.0 26.4
Pm-I	0.07	-0.38	0.30	103.6	214.5	28.8
Pm-II	0.05	-0.35	0.30	87.8	167.3	25.4
Pg-I	0.10	-0.39	0.29	94.9	173.5	24.9
Pg-II	0.13	-0.37	0.24	91.4	162.5	25.4
perhydro-3a,6a,9a-triazaphenalene	0.15	-0.35	0.13	100 ^a	-	2.25 ^a

^aExperimental NMR chemical shift values¹⁵

The dehydration of all these isomers (NC⁺)_n upon geometry optimization converges to the planar form (Figure 1b) as expected. This positively charged lattice structure is isoelectronic to graphene, but the reduced symmetry opens the band-gap (3.09eV) similar to hex-BN nanosheet.²³ (See S4 of the Supporting Information).

The variations in C-N, C-H distances and flattening of nitrogen observed in the optimized geometry along with the energetic preferences of conformers and the projected DOS corresponding to the split-off bands, all clearly points out to the dominant role of anomeric effect in azagraphanes. The preference for anomeric delocalization of the N: lone pair for σ^*_{C-N} over σ^*_{C-H} makes subtle differences in the energetics of different conformers compared to graphane. The consistent domination of H-DOS over C-DOS in the split-off region in all the isomers reveal their hydridic nature. Despite the anomeric delocalization, the existence of split-off bands in all these azagraphane isomers indicate high reactivity of the N: lone pairs. Though, the observed band-gap is too wide for semiconducting applications, the existence of multiple active sites on the azagraphane surface makes it an ideal organocatalyst awaiting discovery.

COMPUTATIONAL METHODS

Calculations on all the nanosheets are performed within the framework of density functional theory (DFT) as implemented in the Cambridge Ab-initio Serial Total energy package (CASTEP), available in the Materials Studio software.²⁴ We employed non-local corrected generalized gradient approximation²⁵ based on the Perdew-Burke-Ernzerhof²⁶ (PBE) formulation and Local Density Approximation²⁷ with CA-PZ (Ceperley and Alder data as parameterized by Perdew and Zunger)²⁸ functional along with ultrasoft pseudo potentials with the plane-wave cut-off of 600eV in a Monkhorst-Pack²⁹ 10x10x1 k-point mesh. The adjacent sheets are kept 25Å away to avoid all possible interactions. The individual atom positions as well as lattice parameters are simultaneously optimized to arrive at the well

converged geometries with the chosen cut-off values for energy ($5.0e^6$ eV) and forces ($0.01eV/\text{\AA}$). Compared to GGA, LDA geometries show consistent shortening of C-N bonds (~ 0.02 \AA), lengthening of C-H bonds (~ 0.01 \AA) and reduction in pyramidalization angles in the range $10^\circ - 0.5^\circ$. However the trends of all the geometrical parameters across various isomeric phases are well correlated in both methodologies resulting in similar relative energies. NMR shielding tensors were computed with the same code using the gauge including projector-augmented plane-wave (GIPAW) method.³⁰

ACKNOWLEDGEMENTS

This research was supported by Department of Science and Technology (DST), India. PDP thanks the DST for the Young Scientist Fellowship (2007-10).

Notes and references

^a Chemical Information Sciences lab, Department of chemistry, Pondicherry university, Puducherry, 605014. India.

E-mail: mmbkr.che@pondiuni.edu.in

Electronic Supplementary Information (ESI) available: Optimised geometries of azagraphane isomers using LDA and GGA methods, band structure of $(NC^+)_n$, optimized lattice parameters and fractional coordinates of all the discussed nanosheets. See DOI: 10.1039/c000000x/

1. D. C. Elias, R. R. Nair, T. M. Mohiuddin, S. V. Morozov, P. Blake, M. P. Halsall, A. C. Ferrari, D. W. Boukhvalov, M. I. Katsnelson, A. K. Geim, K. S. Novoselov, *Science*, 2009, **323**, 610.
2. L. B. Ebert, J. I. Brauman, R. A. Huggins, *J. Am. Chem. Soc.*, 1974, **96**, 7841.
3. M. Pumera, C. H. A. Wong, *Chem. Soc. Rev.*, 2013, **42**, 5987.
4. J. J. Novoa, P. Constans, M.-H. Whangbo, *Angew. Chem., Int. Ed.*, 1993, **32**, 588.
5. J. M. Erhardt, J. D. Wuest, *J. Am. Chem. Soc.*, 1980, **102**, 6363.
6. P. Brunet, J. D. Wuest, *J. Org. Chem.*, 1996, **61**, 2020.
7. W. Kantlehner, H. J. Lehmann, R. Stieglitz, *Arkivoc*, 2012, **2012**, 442.
8. G. A. Olah, *Angew. Chem. Int. Ed.*, 1993, **32**, 767.
9. F. H. Westheimer, *Coenzyme Cofactors*, 1987, **10**, 253.
10. R. K. Thauer, A. R. Klein, G. C. Hartmann, *Chem. Rev.*, 1996, **96**, 3031.
11. L. Wei, Y. Shao, M. Zhou, H. W. Hu, G. Y. Lu, *Org. Biomol. Chem.*, 2012, **10**, 8484.
12. T. J. Atkins, *J. Am. Chem. Soc.*, 1980, **102**, 6364.
13. M. Khazaei, Y. Liang, M. S. Bahrany, F. Pichierri, K. Esfarjani, Y. Kawazoe, *J. Phys.: Condens. Matter*, 2011, **23**, 405403/1.
14. J. M. Erhardt, E. R. Grover, J. D. Wuest, *J. Am. Chem. Soc.*, 1980, **102**, 6365.
15. G. R. Weisman, V. Johnson, R. E. Fiala, *Tetrahedron Lett.*, 1980, **21**, 3635.
16. M. H. F. Sluiter, Y. Kawazoe, *Phys. Rev. B*, 2003, **68**, 085410/10.
17. S. Jorge, C. Ajay, B. Greg, *Phys. Rev. B* 2007, **75**, 153401/1.
18. A. Bhattacharya, S. Bhattacharya, C. Majumder, G. P. Das, *Phys. Rev. B*, 2011, **83**, 033404/1.
19. X. D. Wen, L. Hand, V. Labet, T. Yang, R. Hoffmann, N. W. Ashcroft, A. R. Oganov, A. O. Lyakhov, *Proc. Natl. Acad. Sci. USA*, 2011, **108**, 6833.
20. D. K. Samarakoon, X.-Q. Wang, *ACS Nano*, 2009, **3**, 4017.
21. C. He, C. X. Zhang, L. Z. Sun, N. Jiao, K. W. Zhang, J. Zhong, *Phys. Status Solidi RRL*, 2012, **6**, 427.
22. P. D. Pancharatna, M. M. Balakrishnarajan, E. D. Jemmis, R. Hoffmann, *J. Am. Chem. Soc.*, 2012, **134**, 5916.
23. A. Nag, K. Raidongia, K. P. S. S. Hembram, R. Datta, U. V. Waghmare, C. N. R. Rao, *ACS Nano*, 2010, **4**, 1539.
24. M. D. Segall, J. D. L. Philip, M. J. Probert, C. J. Pickard, P. J. Hasnip, S. J. Clark, M. C. Payne, *J. Phys.: Condens. Matter*, 2002, **14**, 2717.
25. J. P. Perdew and Y. Wang, *Phys. Rev. B*, 1992, **45**, 13244.
26. J. P. Perdew, K. Burke and M. Ernzerhof, *Phys. Rev. Lett.*, 1996, **77**, 3865.
27. W. Kohn and L. J. Sham, *Phys. Rev.* 1965, **140**, A1133.
28. D. M. Ceperley and B. J. Alder, *Phys. Rev. Lett.* 1980, **45**, 566.
29. H. J. Monkhorst and J. D. Pack, *Phys. Rev. B*, 1976, **13**, 5188.
30. C. J. Pickard and F. Mauri, *Phys. Rev. B* 2001, **63**, 245101.